Supplementary Information for

Construction of covalent organic frameworks via Mannich reaction at room temperature for light-driven oxidative hydroxylation of Arylboronic acids

Jian-Cheng Wang†*, Ting Sun†, Jun Zhang, Zhi Chen, Jia-Qi Du, Jing-Lan Kan and Yu-Bin Dong*

College of Chemistry, Chemical Engineering and Materials Science, Collaborative Innovation Centre of Functionalized Probes for Chemical Imaging in Universities of Shandong, Key Laboratory of Molecular and Nano Probes, Ministry of Education, Shandong Normal University, Jinan 250014, P. R. China.
E-mail: wangjiancheng1003@163.com, yubindong@sdnu.edu.cn (Y.B. Dong).
†These authors contributed equally.

Contents

1. General information

All the chemicals were obtained from commercial sources and used without further purification. All characterization tests were carried out through Analysis and Test Center of College of Chemistry, Chemical Engineering and Materials Science, Shandong Normal University. Infrared (IR) spectra were obtained in the 400-4000 cm^{-1} range using a Bruker ALPHA FT-IR Spectrometer. ^{1}H NMR data were collected on an AM-400 spectrometer. Chemical shifts are reported in δ relative to TMS. MS spectra were obtained by Bruker maxis ultra-high resolution-TOF MS system. Thermogravimetric analyses (TGA) were carried out on a TA Instrument Q5 simultaneous TGA under flowing nitrogen at a heating rate of 5 °C/min. PXRD patterns were obtained on D8 Advance X-ray powder diffractometer with Cu Kα radiation (λ = 1.5405 Å). HR-TEM (High Resolution Transmission Electron Microscopy) analyses were performed on a JEOL 2100 Electron Microscope at an operating voltage of 200 kV. The total surface areas of the COFs were measured by the BET (Brunauer Emmer Teller) isotherms using N_2 adsorption at 77 K and this was done on the Micromeritics ASAP 2020 sorption/desorption analyzer. ^{13}C CP-MAS solid-state NMR spectra were recorded on a MERCURY plus 400 spectrometers operating at resonance frequencies of 400M Hz and the sample rotation frequency is 8.0-10.2 kHz. ^{15}N CP-MAS solid-state NMR spectra were recorded on a MERCURY plus 400 spectrometers operating at resonance frequencies of 400M Hz and the sample rotation frequency is 12 kHz. The scanning electron microscopy (SEM) micrographs were recorded on a Gemini Zeiss Supra TM scanning electron microscope equipped with energy-dispersive X-ray detector (EDX). Ultraviolet–visible (UV−vis) absorption spectra were recorded on a Shimadzu UV-2600 Double Beam UV−vis Spectrophotometer. The model of LED lamp is PL-SX100A. Electron paramagnetic resonance (EPR) spectra was measured by Bruker A300 EPR Spectroscopy.

2. Synthesis and characterization of model compound 1,3-diphenyl-3-(phenylamino) propan-1-one

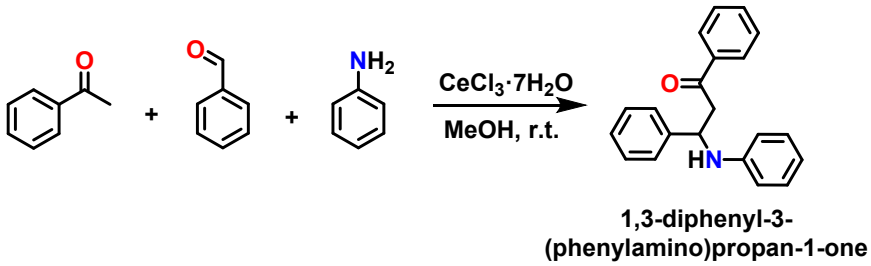

1,3-diphenyl-3-(phenylamino)propan-1-one

Scheme S1 Synthesis of **1,3-diphenyl-3-(phenylamino) propan-1-one**.

A mixture of acetone (4.0 mmol), benzaldehyde (1.0 mmol) and aniline (1.0 mmol) was stirred at 25 ℃ for 0.5 h in methanol (5 mL). Then, $CeCl_3·7H_2O$ (cerium hydrate) (50 mol% as catalyst) was added to the mixture and the mixture was continuously stirred at 25 ℃. The progress of the reaction was monitored by TLC. After reaction, the solvent was removed by vacuum evaporation to afford the crude product and the crude product was purified by recrystallization with ethanol in 86% yield. IR (KBr pellet cm^{-1}): 3385 (s), 3052 (vw), 2918 (vw), 2877 (vw), 671 (vs), 1600 (s), 1510 (s), 1448 (w), 1369 (vw), 1291 (s), 1221 (w), 1176 (vw), 1116 (vw), 1068 (vw), 1002 (vw), 920 (vw), 862 (vw), 768 (w), 748 (s), 701 (s), 689 (s), 622 (w), 579 (w), 543 (w), 510 (w). ^{1}H NMR (400 MHz, $CDCl_3$) δ 7.83 (d, J = 8.0 Hz, 2H), 7.49 (s, 1H), 7.37 (dd, J = 10.0, 3.4 Hz, 4H), 7.24 (d, J = 8.0 Hz, 2H), 7.20 -7.12 (m, 2H), 7.02 (s, 2H), 6.61 (s, 1H), 6.51 (d, J = 8.0 Hz, 2H), 4.93 (s, 1H), 3.45 (s, 1H), 3.39 (s, 1H). ^{13}C NMR (100 MHz, $CDCl_3$) δ 198.44, 146.58, 142.67, 136.65, 133.47, 129.14, 128.85, 128.73, 128.23, 127.45, 126.48, 118.16, 114.26, 55.12, 46.26. HRMS (ESI, m/z) calcd. For $C_{21}H_{19}NO$ $[M+H]^+$: 302.1537, found 302.1530.

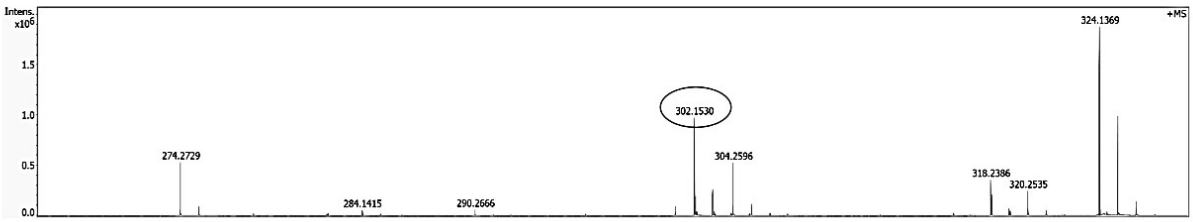

Fig. S1 HR-MS of **1,3-diphenyl-3-(phenylamino) propan-1-one**.

3. Synthesis and characterization of TAD-COF

A mixture of 4,4',4''-(1,3,5-triazine-2,4,6-triyl) tribenzaldehyde (TATB) (0.05 mmol, 19.7 mg), acetophenone (0.60 mmol, 70 μL) and 4,4'-diaminodiphenyl (0.075 mmol, 13.8 mg) were stirred at 25 °C for 30 min in a mixture of methanol (2.6 mL) and acetonitrile (1.3 mL) in a round-bottomed flask. Then, cerium chloride heptahydrate (28.0 mg, 0.075 mmol) was added into the mixture and the mixture was stirred at room temperature for 7 days. The obtained precipitate was collected by centrifugation and washed with N, N-dimethyl formamide, ethanol and ether, respectively. After dried in vacuo overnight, **TAD-COF** was obtained as the yellowish-brown crystalline powder in 75.1% yield (36.8 mg). IR (KBr pellet cm^{-1}): 3385 (w), 3026 (w), 1699 (w), 1670 (w), 1621 (w), 1574 (w), 1511 (vs), 1412 (w), 1361 (s), 1293 (w), 1194 (w), 1104 (vw), 1015 (vw), 810 (s), 742 (vw), 545 (w).

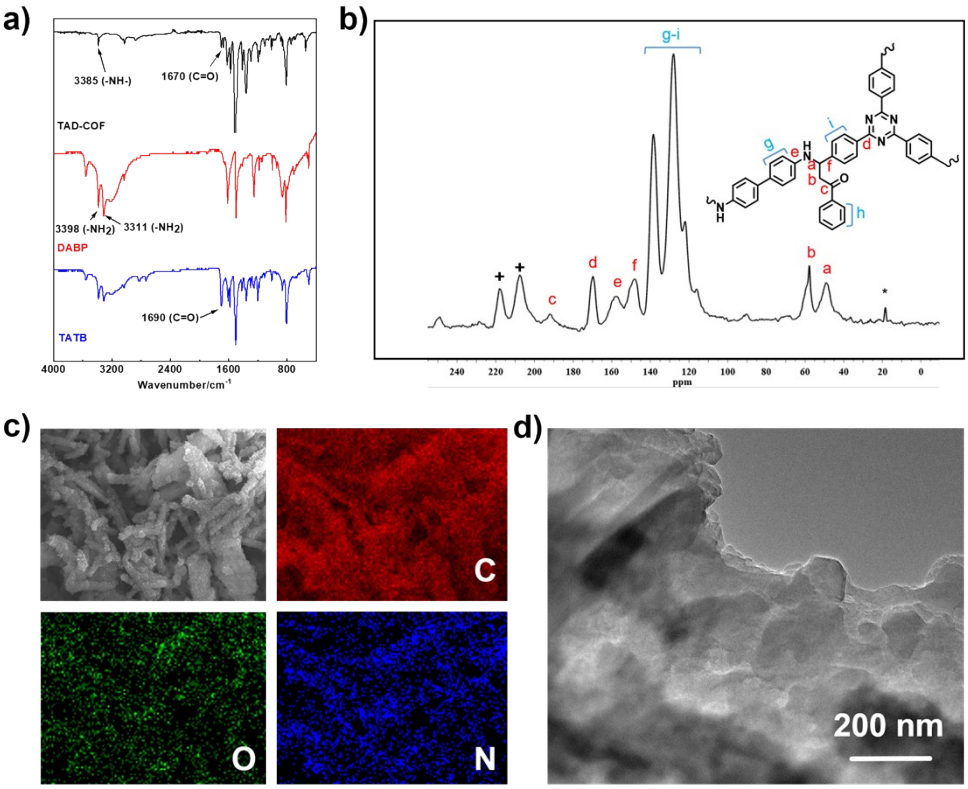

Fig. S2 a) The FT-IR spectra of **TAD-COF** and its monomers. The Fourier transform infrared (FT-IR) spectra showed all characteristic peaks, such as 1670 cm^{-1} for [−C=O], 3385 cm^{-1} for [−NH−] stretching vibrations, which suggested the formation of **TAD-COF** through the Mannich condensation reaction. b) The solid-state ^{13}C-MAS NMR spectrum of **TAD-COF**, δ (ppm): 193.4, 169.7, 157.3, 147.8, 138.4, 128.0, 122.0, 57.7, 49.8. The plus sign may be the unreacted terminal aldehyde carbon signal of COF materials. Asterisks denote spinning sidebands.[1, 2] The formation of **TAD-COF** was verified by the

existence of the keto and aliphatic carbon in **TAD-COF** through the corresponding resonances at 193.4, 57.7, 49.8 ppm, respectively. c) SEM-EDX images of **TAD-COF** d) TEM image of **TAD-COF**.

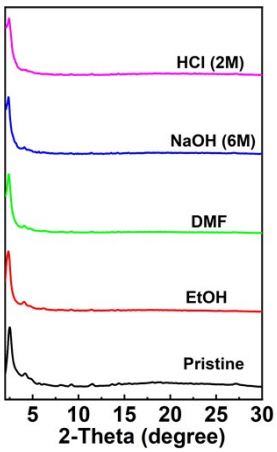

Fig. S3 Stability examination in different media. The PXRD patterns indicated that the crystallinity and structural integrity of **TAD-COF** were well maintained after it was soaked in different media for 24 h.

Table S1. Fractional atomic coordinates for the unit cell of **TAD-COF**

Py-O-COF AA stacking mode, space group: *P6*

$a = b = 42.5183$ Å, $c = 3.7231$ Å

$\alpha = \beta = 90°$, $\gamma = 120°$

Aotm	x	y	z
C1	0.29871	-0.36209	0.6554
N2	0.32752	-0.36768	0.65478
C3	0.26112	-0.39332	0.63423
C4	0.23105	-0.38865	0.68833
C5	0.19568	-0.41789	0.64941
C6	0.18907	-0.4528	0.55303
C7	0.21967	-0.45707	0.50205
C8	0.25494	-0.42795	0.54427
C9	0.14954	-0.48398	0.49918
N10	0.12843	-0.47032	0.30728
C11	0.14572	-0.51853	0.3136
C12	0.14786	-0.54693	0.54155
O13	0.17765	-0.54273	0.61612
C14	0.11503	-0.58161	0.64671
C15	0.09158	-0.48052	0.39269
C16	0.08389	-0.4546	0.5358

C17	0.04791	-0.46245	0.57415
C18	0.01897	-0.4964	0.46804
C19	0.02678	-0.52245	0.32939
C20	0.0627	-0.51431	0.28628
C21	0.0808	-0.58431	0.67813
C22	0.05038	-0.61691	0.78204
C23	0.05371	-0.64728	0.85644
C24	0.08752	-0.64502	0.82859
C25	0.11803	-0.6124	0.72557
H26	0.4824	0.69973	1.42239
H27	0.23478	-0.36226	0.75762
H28	0.17346	-0.41268	0.68397
H29	0.27748	-0.43251	0.49677
H30	0.13645	-0.49265	0.7558
H31	0.14226	-0.44718	0.14892
H32	0.16697	-0.50961	0.10721
H33	0.11946	-0.53269	0.17418
H34	0.10586	-0.42802	0.61055
H35	0.04269	-0.44182	0.68138
H36	0.00516	-0.54835	0.2336
H37	0.0676	-0.53378	0.15039
H38	0.07771	-0.56101	0.63423
H39	0.02427	-0.6185	0.80803
H40	0.03015	-0.67249	0.93818
H41	0.09012	-0.66852	0.88806
H42	0.14395	-0.61134	0.70564

4. The product characterization for optimization of reaction conditions for the model oxidation hydroxylation reaction of phenylboronic acid (Table 1)

In oxygen, a mixture of phenylboronic acid (0.50 mmol), DIPEA (N, N-diisopropylethylamine), **TAD-COF** (7-15 mg), and solvent (2.5 mL) was stirred at 25 °C under blue LED (460 nm, 40 mW/cm^2) irradiation. TLC (thin-layer chromatography) was used to monitor the reaction progress. After completion of the reaction, the catalyst was recovered by centrifugation and the obtained crude products were purified by column on silica gel using dichloromethane and methanol as eluent to provide the corresponding products. The product was characterized by ^{13}H NMR, ^{13}C NMR and HRMS

measurements.

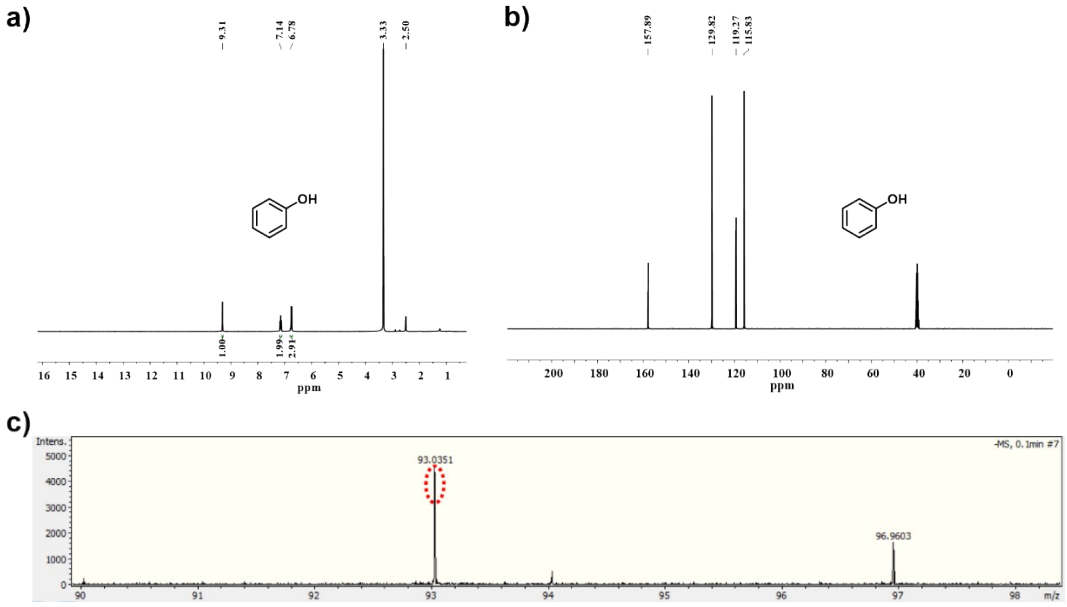

Fig. S4 (a) ^{1}H NMR spectrum of the model reaction product. ^{1}H NMR (400 MHz, DMSO-d_6) δ 9.31 (s, 1H), 7.14 (s, 2H), 6.78 (s, 3H). (b) ^{13}C NMR spectrum of the model reaction product. ^{13}C NMR (101 MHz, DMSO-d_6) δ 157.89, 129.82, 119.27, 115.83. (c) MS spectrum of the model reaction product. HRMS (ESI): *m/z* [M-H]$^-$, Calcd for $C_6H_5O^-$ 93.0349, found 93.0351.

5. Leaching test of TAD-COF-catalyzed photo-induced oxidative hydroxylation reaction of phenylboronic acid

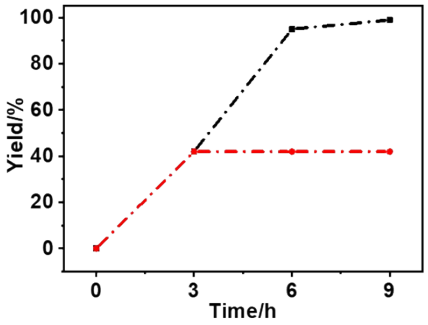

Fig. S5 Reaction time examination (black line) and leaching test (red line). The solid catalyst was filtrated from the reaction solution after 3 h, and the filtrate was transferred to a new vial and the reaction was carried out under the same conditions for an additional 6 h.

6. Summary and comparison of the reported metal-free organic porous materials for the photocatalytic oxidative hydroxylation of the arylboronic acids

Table S2. Summary and comparison of the reported metal-free organic porous materials for the photocatalytic oxidative hydroxylation of the arylboronic acids

Catalyst	Light Source	T/°C	Time/h	Oxidant	Yield/%	Ref.
PCP-MF	white LEDs	25	10	O_2	94	3
Cz-POF-1	fluorescence lamp	25	24	air	94	4
LZU-190-COF	white LEDs	25	48	air	99	1

BBO-COF	white LEDs	25	48	air	99	5
TFB-BMTH-COF	white LEDs	25	24	O_2	99	6
Cy-N3-COF	blue LEDs	25	6	O_2	99	7
TAD-COF	**460 nm LEDs**	**25**	**9**	**O_2**	**99**	**This work**

7. Products characterization for the TAD-COF-catalyzed photo-induced oxidative hydroxylation reaction (Table 2)

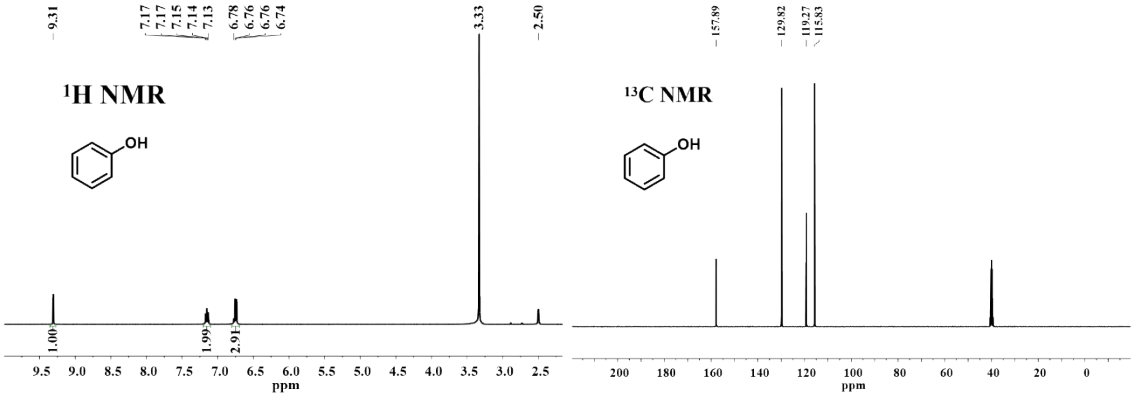

Phenol (2a): The product is isolated by column chromatography on silica gel as white solid (46.5 mg, isolated yield: 99%). ^{1}H NMR (400 MHz, DMSO-d_6) δ 9.31 (s, 1H), 7.15 (m, 2H), 6.76 (dd, *J*=8.0 Hz, 3H). ^{13}C NMR (101 MHz, DMSO-d_6) δ 157.8, 129.8, 119.2, 115.8. HRMS (ESI) m/z [M-H]$^-$ calcd for $C_6H_5O^-$ 93.0349, found 93.0351.

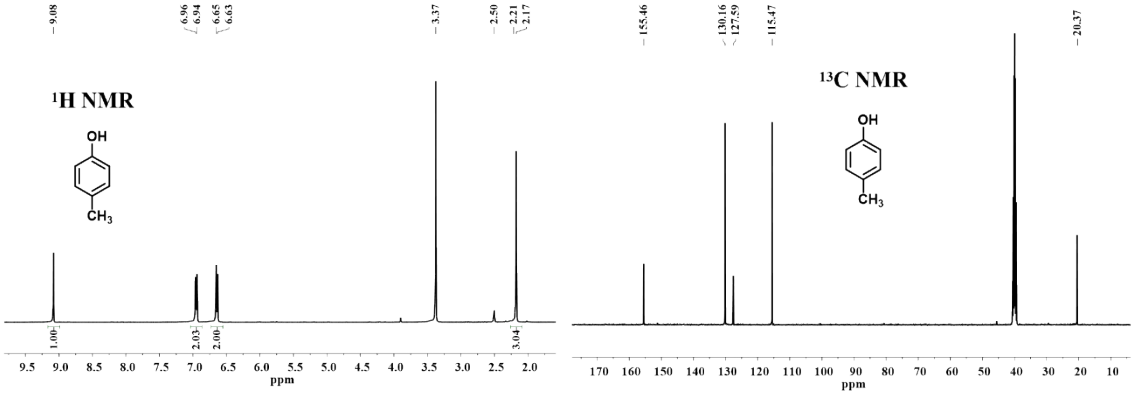

p-Cresol (2b): The product is isolated by column chromatography on silica gel as colorless liquid (44.7 mg, isolated yield: 83%). ^{1}H NMR (400 MHz, DMSO-d_6) δ 9.08 (s, 1H), 6.95 (d, *J*=8.0 Hz, 2H), 6.62 (d, *J*=8.0 Hz, 2H), 2.19 (s, 3H). ^{13}C NMR (101 MHz, DMSO-d_6) δ 155.4, 130.1, 127.5, 115.4, 20.3. HRMS (ESI) m/z [M-H]$^-$ calcd for $C_7H_7O^-$ 107.0505, found 107.0501.

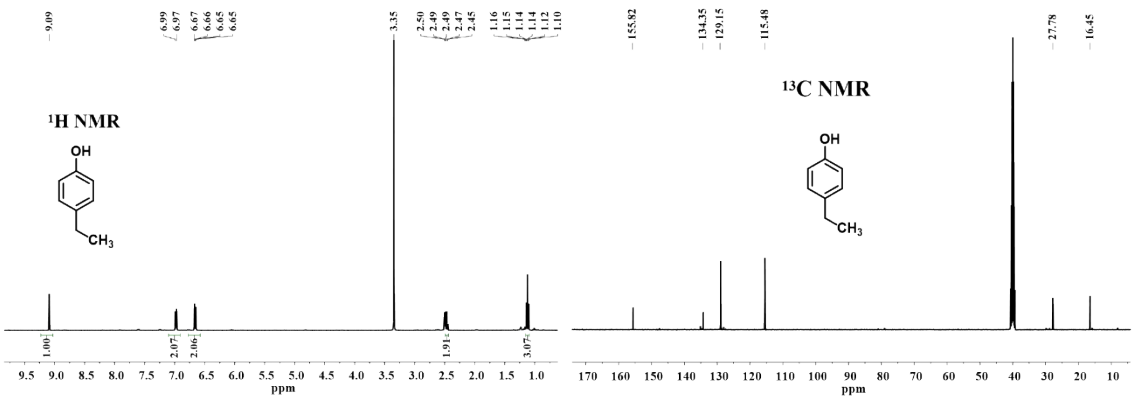

4-Ethylphenol (2c): The product is isolated by column chromatography on silica gel as colorless liquid (55.3 mg, isolated yield: 91%). ^{1}H NMR (400 MHz, DMSO-d_6) δ 9.09 (s, 1H), 6.98 (d, J=8.0 Hz, 2H), 6.66 (d, J=8.0 Hz, 2H), 2.46 (t, J=8.0 Hz, 2H), 1.15 (d, 3H). ^{13}C NMR (101 MHz, DMSO-d_6) δ 155.8, 134.3, 129.1, 115.4, 27.7, 16.4. HRMS (ESI) m/z [M-H]$^-$ calcd for $C_8H_9O^-$ 121.0662, found 121.0632.

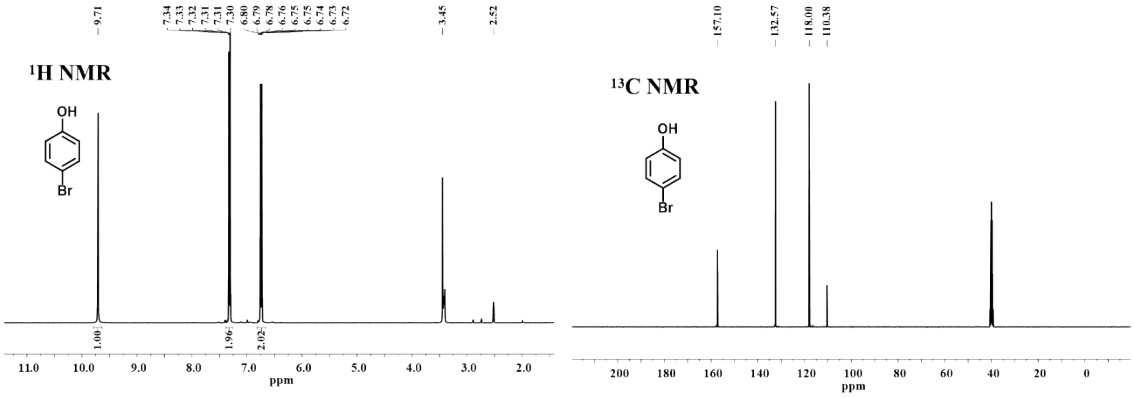

4-Bromophenol (2d): The product is isolated by column chromatography on silica gel as brown solid (83.1 mg, isolated yield: 97%). ^{1}H NMR (400 MHz, DMSO-d_6) δ 9.71 (s, 1H), 7.32 (m, 2H), 6.76 (m, 2H). ^{13}C NMR (101 MHz, DMSO-d_6) δ 157.1, 132.5, 118.0, 110.3. HRMS (ESI) m/z [M-H]$^-$ calcd for $C_6H_4BrO^-$ 170.9454, found 170.9425.

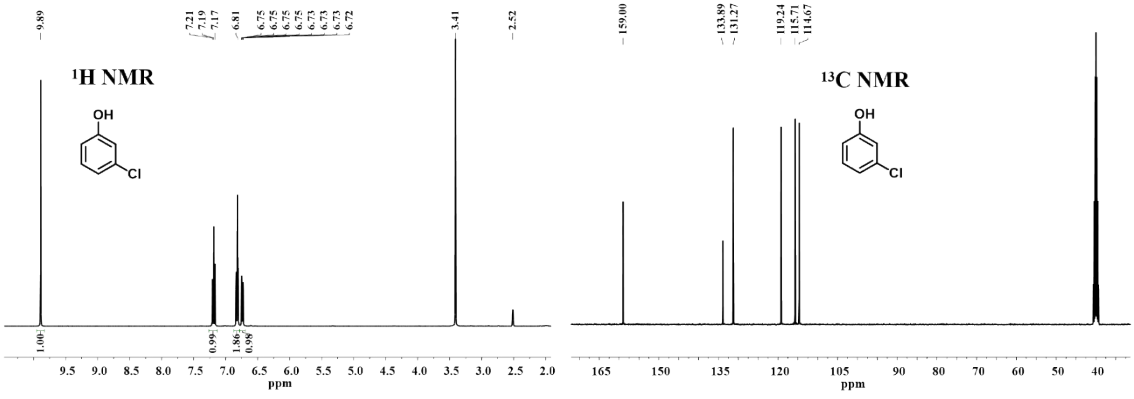

3-Chlorophenol (2e): The product is isolated by column chromatography on silica gel as white solid (61.3 mg, isolated yield: 96%). ^{1}H NMR (400 MHz, DMSO-d_6) δ 9.89 (s, 1H), 7.27–7.11 (m, 1H), 6.86–6.79 (m, 2H), 6.74 (dd, J=8.0 Hz, 1H). ^{13}C NMR (101 MHz, DMSO-d_6) δ 159.0, 133.8, 131.2, 119.2, 115.7, 114.6. HRMS (ESI) m/z [M-H]$^-$ calcd for $C_6H_4ClO^-$ 126.9959, found 126.9940.

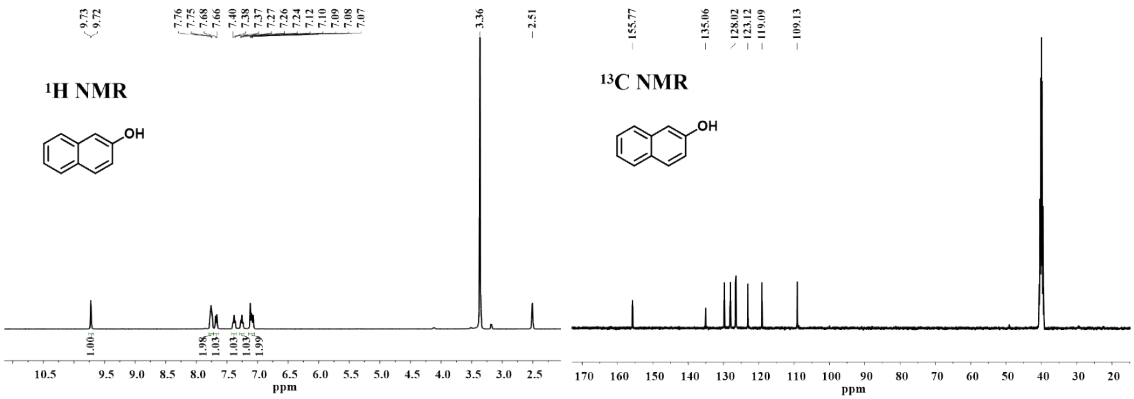

Naphthalen-2-ol (2f): The product is isolated by column chromatography on silica gel as yellow solid (69.1 mg, isolated yield: 96%). ^{1}H NMR (400 MHz, DMSO-d_6) δ 9.72 (d, 1H), 7.75 (d, J=8.0 Hz, 2H), 7.67 (d, J=8.0 Hz, 1H), 7.38 (t, J=8.0 Hz, 1H), 7.26 (t, J=8.0 Hz, 1H), 7.15–7.05 (m, 2H). ^{13}C NMR (101 MHz, DMSO-d_6) δ 155.7, 135.0, 129.7, 128.2, 128.0, 126.5, 126.4, 123.1, 119.0, 109.1. HRMS (ESI) m/z [M-H]$^-$ calcd for $C_{10}H_7O^-$ 143.0505, found 143.0475.

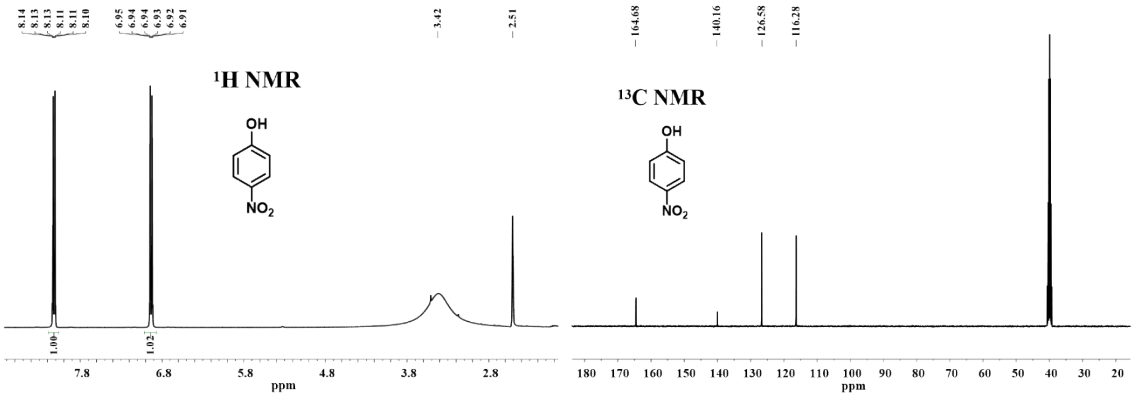

4-Nitrophenol (2g): The product is isolated by column chromatography on silica gel as yellow solid (67.4 mg, isolated yield: 97%). ^{1}H NMR (400 MHz, DMSO-d_6) δ 8.13 (d, J=8.0 Hz, 2H), 6.93 (d, J=8.0 Hz, 2H). ^{13}C NMR (101 MHz, DMSO-d_6) δ 164.6, 140.1, 126.5, 116.2. HRMS (ESI) m/z [M-H]$^-$ calcd for $C_6H_4NO_3^-$ 138.0191, found 138.0131.

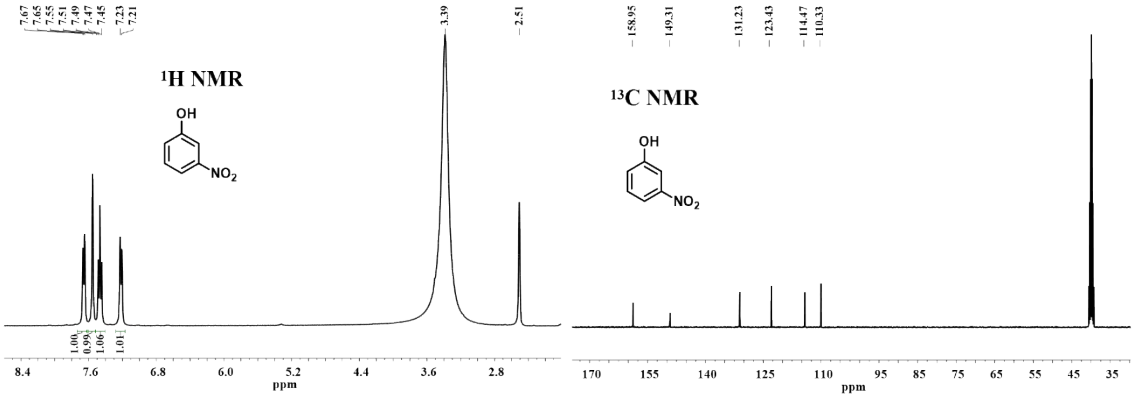

3-Nitrophenol (2h): The product is isolated by column chromatography on silica gel as yellow solid (66.7 mg, isolated yield: 96%). ^{1}H NMR (400 MHz, DMSO-d_6) δ 7.66 (d, J=8.0 Hz, 1H), 7.53 (d, J=8.4 Hz, 1H), 7.47 (t, J=8.2 Hz, 1H), 7.22 (d, J=6.8 Hz, 1H). ^{13}C NMR (101 MHz, DMSO-d_6) δ 158.9, 149.3, 131.2, 123.4, 114.4, 110.3. HRMS (ESI) m/z [M-H]$^-$ calcd for $C_6H_4NO_3^-$ 138.0191, found 138.0127.

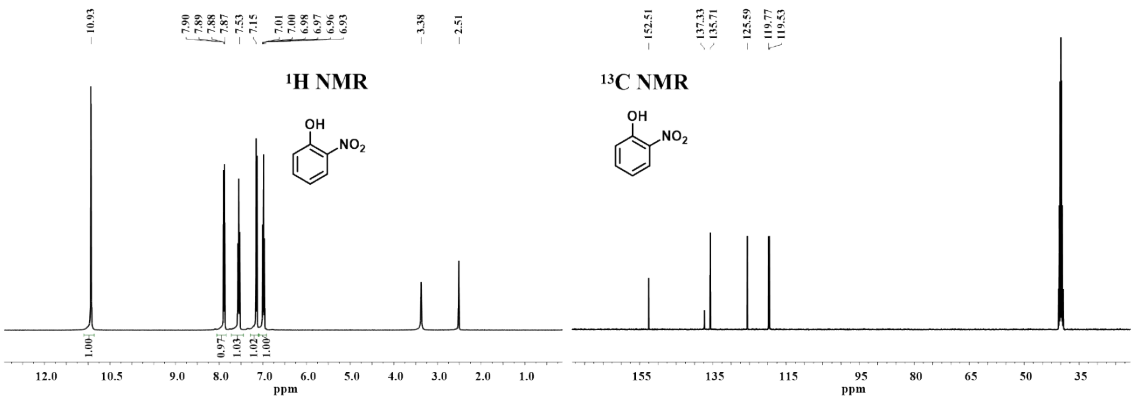

2-Nitrophenol (2i): The product is isolated by column chromatography on silica gel as yellow solid (62.4 mg, isolated yield: 90%). ^{1}H NMR (400 MHz, DMSO-d_6) δ 10.93 (s, 1H), 7.89 (dd, J=8.4, 1H), 7.55 (dd, J=8.8 Hz, 1H), 7.22–7.10 (m, 1H), 6.98 (dt, J=7.8 Hz, 1H). ^{13}C NMR (101 MHz, DMSO-d_6) δ 152.5, 137.3, 135.7, 125.5, 119.7, 119.5. HRMS (ESI) m/z [M-H]$^-$ calcd for $C_6H_4NO_3^-$ 138.0191, found 138.0115.

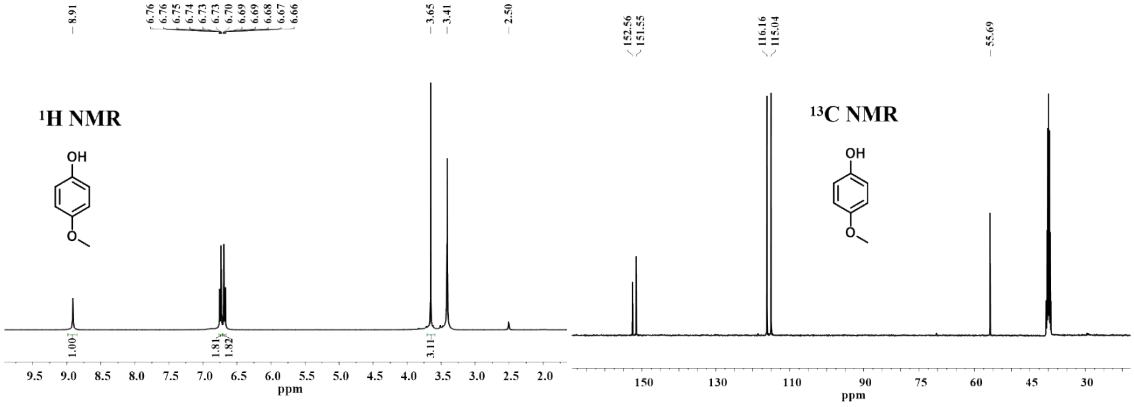

4-Methoxyphenol (2j): The product is isolated by column chromatography on silica gel as yellow solid (58.2 mg, isolated yield: 94%). ^{1}H NMR (400 MHz, DMSO-d_6) δ 8.91 (s, 1H), 6.77–6.72 (m, 2H), 6.71–6.65 (m, 2H), 3.70–3.60 (m, 3H). ^{13}C NMR (101 MHz, DMSO-d_6) δ 152.5, 151.5, 116.1, 115.0, 55.6. HRMS (ESI) m/z [M-H]$^-$ calcd for $C_7H_7O_2^-$ 123.0454, found 123.0428.

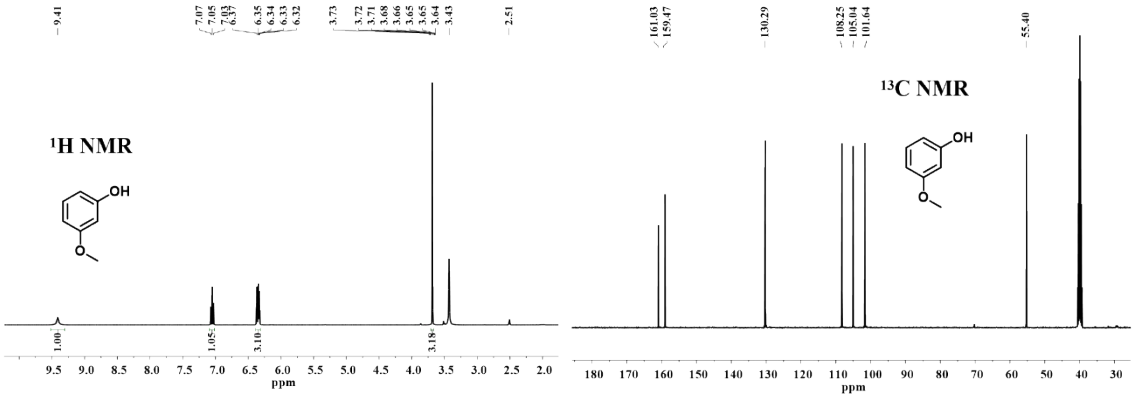

3-Methoxyphenol (2k): The product is isolated by column chromatography on silica gel as yellow solid (54.2 mg, isolated yield: 88%). ^{1}H NMR (400 MHz, DMSO-d_6) δ 9.41 (s, 1H), 7.11–6.99 (m, 1H), 6.42–6.30 (m, 3H), 3.75–3.64 (m, 3H). ^{13}C NMR (101 MHz, DMSO-d_6) δ 161.0, 159.4, 130.2, 108.2, 105.0, 101.6, 55.4. HRMS (ESI) m/z [M-H]$^-$ calcd for $C_7H_7O_2^-$ 123.0454, found 123.0418.

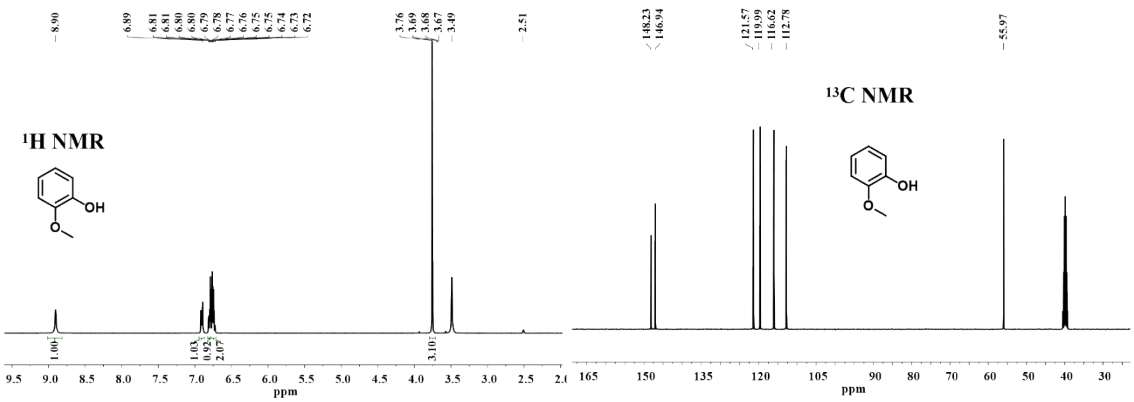

2-Methoxyphenol (2l): The product is isolated by column chromatography on silica gel as yellow solid (55.1 mg, isolated yield: 89%). ^{1}H NMR (400 MHz, DMSO-d_6) δ 8.90 (s, 1H), 6.93–6.88 (m, 1H), 6.82–6.79 (m, 1H), 6.75 (qd, *J*=7.4 Hz, 2H), 3.88–3.64 (m, 3H). ^{13}C NMR (101 MHz, DMSO-d_6) δ 148.2, 146.9, 121.5, 119.9, 116.6, 112.7, 55.9. HRMS (ESI) m/z [M-H]$^-$ calcd for $C_7H_7O_2^-$ 123.0454, found 123.0409.

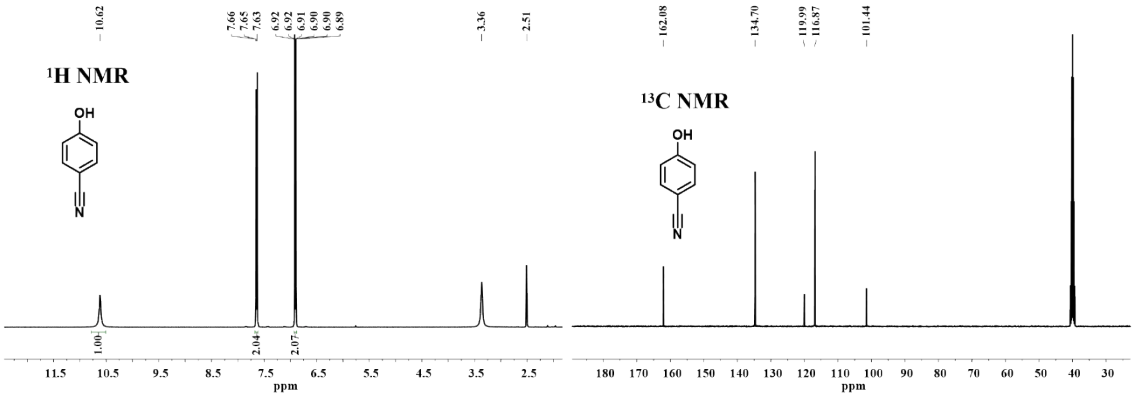

4-Cyanophenol (2m): The product is isolated by column chromatography on silica gel as white solid (56.5 mg, isolated yield: 95%). ^{1}H NMR (400 MHz, DMSO-d_6) δ 10.62 (s, 1H), 7.65 (d, *J*=12.0 Hz, 2H), 6.91 (d, *J*=12.0 Hz, 2H). ^{13}C NMR (101 MHz, DMSO-d_6) δ 162.0, 134.7, 119.9, 116.8, 101.4. HRMS (ESI) m/z [M-H]$^-$ calcd for $C_7H_4NO^-$ 118.0301, found 118.0290.

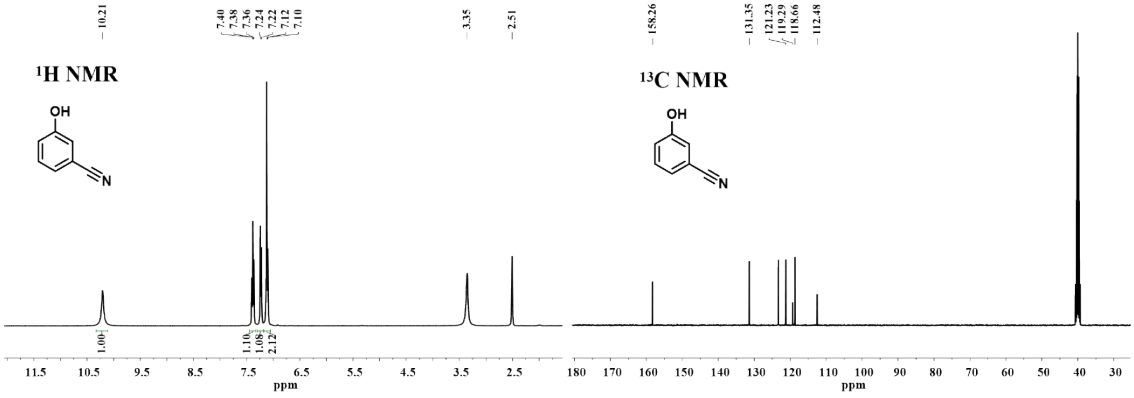

3-Cyanophenol (2n): The product is isolated by column chromatography on silica gel as white solid (54.5 mg, isolated yield: 92%). ^{1}H NMR (400 MHz, DMSO-d_6) δ 10.21 (s, 1H), 7.38 (t, *J*=7.8 Hz, 1H), 7.23 (d, *J*=7.6 Hz, 1H), 7.11 (d, *J*=8.2 Hz, 2H). ^{13}C NMR (101 MHz, DMSO-d_6) δ 158.2, 131.3, 123.2, 121.2, 119.2, 118.6, 112.4. HRMS (ESI) m/z [M-H]$^-$ calcd for $C_7H_4NO^-$ 118.0301, found 118.0323.

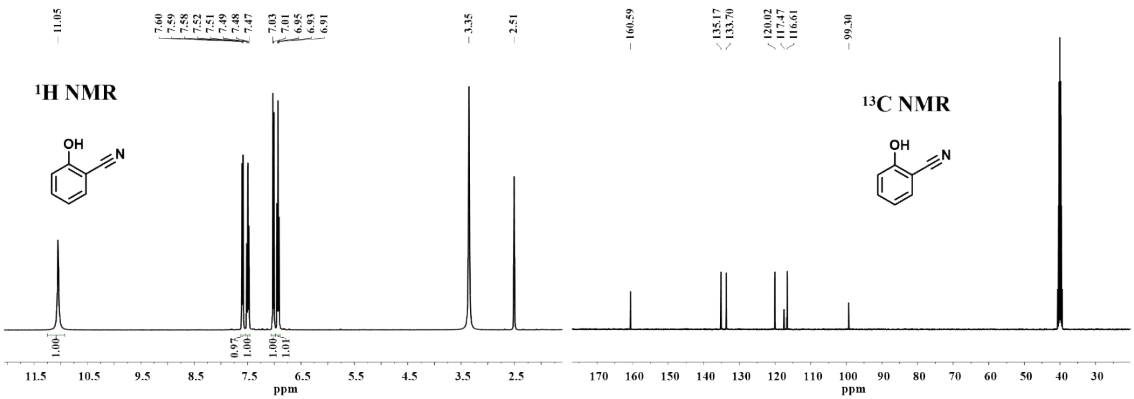

2-Cyanophenol (2o): The product is isolated by column chromatography on silica gel as white solid (57.1 mg, isolated yield: 96%). ^{1}H NMR (400 MHz, DMSO-d_6) δ 11.05 (s, 1H), 7.60 (dd, J=7.8 Hz, 1H), 7.55–7.44 (m, 1H), 7.02 (d, J=8.4 Hz, 1H), 6.93 (t, J=7.6 Hz, 1H). ^{13}C NMR (101 MHz, DMSO-d_6) δ 160.5, 135.1, 133.7, 120.0, 117.4, 116.6, 99.3. HRMS (ESI) m/z [M-H]$^-$ calcd for $C_7H_4NO^-$ 118.0301, found 118.0293.

8. The ESR experiments

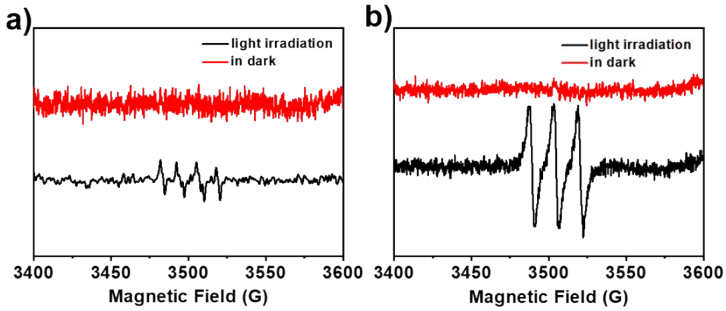

Fig. S6 a) ESR spectrum of the solution of **TAD-COF** (5 mg), DIPEA (5 μL) and DMPO (5 μL) in O_2 atmosphere in CH_3CN (90 μL) in dark (red) and upon irradiation with blue LEDs light for 30 s (black). b) ESR spectrum of the solution of **TAD-COF** (5 mg), DIPEA (5 μL) and TEMP (5 μL) in CH_3CN (90 μL) in dark (red) and upon irradiation with blue LEDs light for 30 s (black).

9. The quenching experiments

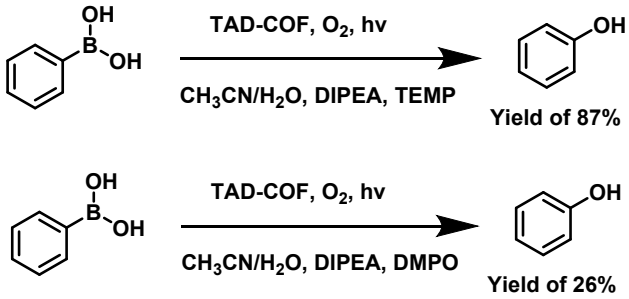

Scheme S2 The quenching experiments using TEMP and DMPO as the scavengers.

10. Synthesis and characterization of DAT-COF

A mixture of 2,5-dimethoxyterephthalaldehyde (DMTP) (0.075 mmol, 14.6 mg), acetophenone (0.60 mmol, 70 μL) and 1,3,5-tris(4-aminophenyl) benzene (TAPB) (0.05 mmol, 17.6 mg) were stirred at 25 ℃

for 30 min in a mixture of methanol (2.0 mL), acetonitrile (0.5 mL) and chloroform (1.5 mL) in a round-bottomed flask. Then, cerium chloride heptahydrate (28.0 mg, 0.075 mmol) was added into the mixture and the mixture was stirred at room temperature for 7 days. The obtained precipitate was collected by centrifugation and washed with N, N-dimethyl formamide, ethanol and ether, respectively. The collected solid was then dried in vacuo overnight to yield **DAT-COF** (39.0 mg, 81.8% yield). IR (KBr pellet cm^{-1}): 3374 (vw), 2936 (vw), 2832 (vw), 1669 (w), 1615 (s), 1593 (s), 1506 (s), 1487 (s), 1465 (s), 1409 (vs), 1289 (s), 1211 (vs), 1181 (vw), 1144 (vw), 1038 (s), 879 (vw), 829 (s), 694 (w).

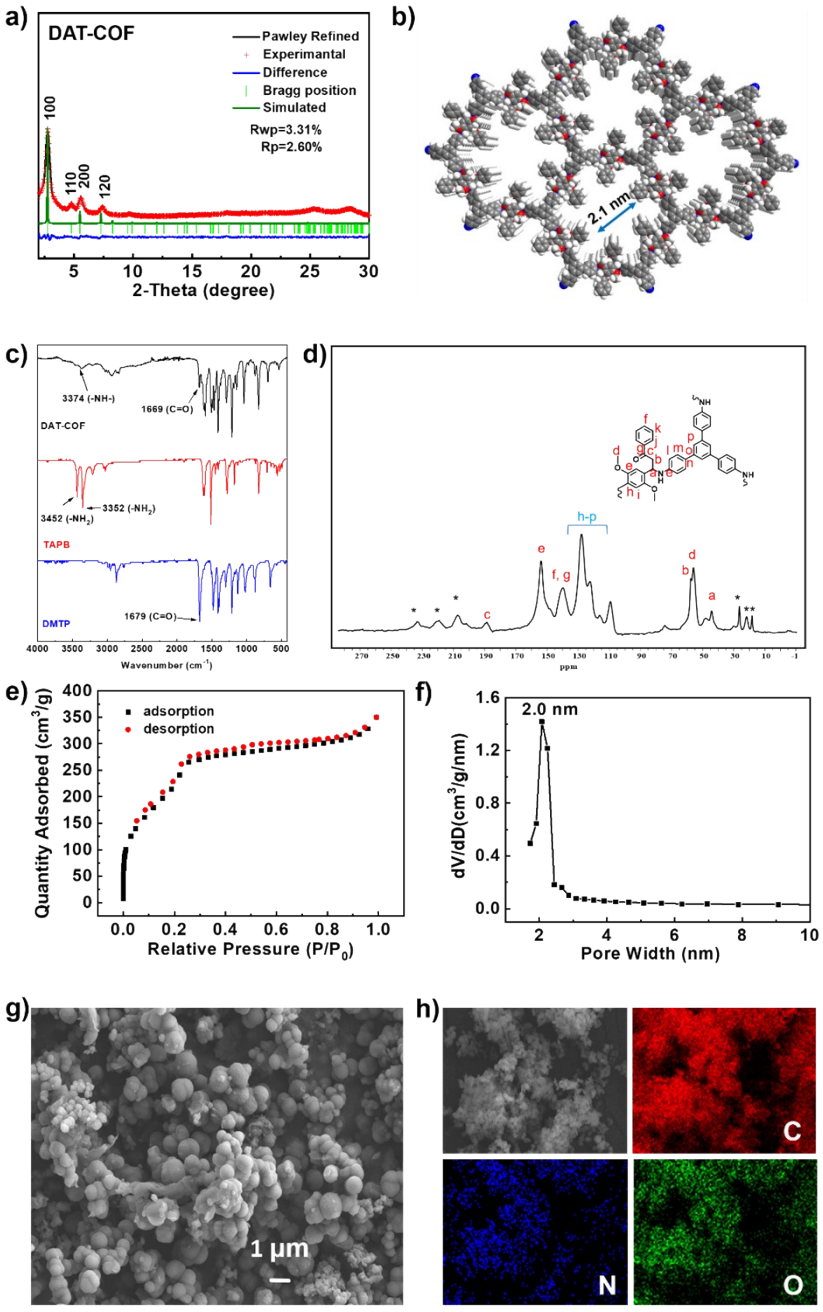

Fig. S7 a) PXRD patterns of **DAT-COF** (AA stacking). b) The top and side views of **DAT-COF** (AA stacking). c) The FT-IR spectra of **DAT-COF** and its part monomers. The FT-IR spectra showed the characteristic peaks such as 1669 cm^{-1} for [−C=O], 3374 cm^{-1} for [−N-H] stretching vibrations, which suggested the formation of **DAT-COF** through Mannich condensation reaction. d) The solid-state ^{13}C-MAS NMR spectrum of **DAT-COF**, δ (ppm): 188.7, 153.7, 139.7, 127.7, 122.2, 109.2, 57.8, 57.5, 44.8. The formation of **DAT-COF** was verified by the existence of the keto and aliphatic carbon in **DAT-COF** through the corresponding resonances at 188.7, 57.8, 57.5, 44.8 ppm, respectively. e) N_2 adsorption isotherms for **DAT-COF** at 77 K. N_2 adsorption at 77 K revealed absorption amounts of **DAT-COF** was 350.0 cm^3/g, and its surface areas calculated on basis of the BET model were determined as 935.0 m^2/g. f) Pore size distribution curve of **DAT-COF**. Pore size distribution curves, calculated from nonlocal density functional theory (NLDFT) analysis, showed that the pore width of **DAT-COF** was centered at ~2.0 nm. g) SEM image of **DAT-COF**. h) SEM-EDX images of **DAT-COF**. i) TEM image of the **DAT-COF**. j) TGA trace of **DAT-COF** measured under nitrogen flow with a heating rate 10 ℃/min up to 800 ℃, which can be stable up to 400 ℃. k) UV-Vis curve of the **DAT-COF** measured in solid state. **DAT-COF** exhibited an absorption maximum at around 365 nm with an absorbance edge at 700 nm. l) Photocurrent response of **DAT-COF**.

Table S3. Fractional atomic coordinates for the unit cell of **DAT-COF**

DAT-COF AA stacking mode, space group: *P6*

$a = b = 37.0976$ Å, $c = 3.5871$ Å

$\alpha = \beta = 90°$, $\gamma = 120°$

Aotm	x	y	z
C1	0.35742	-0.28929	-0.23999
C2	0.30964	-0.37666	-0.2337
C3	0.24302	-0.37418	-0.28998
C4	0.22061	-0.35419	-0.1877
C5	0.17851	-0.37155	-0.2776

C6	0.15719	-0.41015	-0.45821
C7	0.17863	-0.43129	-0.54065
C8	0.2209	-0.41349	-0.46307
N9	0.11562	-0.42679	-0.60067
C10	0.08212	-0.42038	-0.45164
C11	0.09071	-0.37569	-0.57033
C12	0.03935	-0.46151	-0.48151
C13	0.00117	-0.46226	-0.46132
C14	0.03745	-0.50056	-0.43634
C15	0.05673	-0.36808	-0.70785
C16	0.0532	-0.33185	-0.58341
O17	0.03257	-0.3909	-0.94113
C18	0.08875	-0.29351	-0.49749
C19	0.08477	-0.25947	-0.38913
C20	0.04544	-0.26325	-0.3664
C21	0.00999	-0.30106	-0.45338
C22	0.01379	-0.33517	-0.56272
O23	0.07438	-0.50108	-0.34796
C24	0.07225	-0.53788	-0.20079
H25	0.29132	-0.41007	-0.23698
H26	0.23529	-0.32493	-0.03926
H27	0.16354	-0.35399	-0.21182
H28	0.16296	-0.46089	-0.68483
H29	0.2362	-0.42993	-0.56165
H30	0.10791	-0.44838	-0.81556
H31	0.08601	-0.41741	-0.15577
H32	0.11656	-0.362	-0.77084
H33	0.10504	-0.35446	-0.33381
H34	0.11963	-0.28947	-0.52137
H35	0.11223	-0.23007	-0.32375
H36	0.04244	-0.23687	-0.28169
H37	-0.02047	-0.30395	-0.43643

H38	-0.01405	-0.36421	-0.62999
H39	0.10284	-0.52951	-0.07682
H40	0.06549	-0.56125	-0.42105
H41	0.04822	-0.55173	0.01789
H42	0.00059	-0.43409	-0.44094

11. Synthesis and characterization of TAT-COF

A mixture of 4,4',4"-(1,3,5-triazine-2,4,6-triyl) tribenzaldehyde (TATB) (0.05 mmol, 19.7 mg), acetophenone (0.60 mmol, 70 μL) and 1,3,5-tris(4-aminophenyl) benzene (TAPB) (0.05 mmol, 17.6 mg) were stirred at 25 ℃ for 30 min in a mixture of methanol (2.0 mL) and chloroform (2.0 mL) in a round-bottomed flask. Then, cerium chloride heptahydrate (28.0 mg, 0.075 mmol) was added into the mixture and the mixture was stirred at room temperature for 7 days. The obtained precipitate was collected by centrifugation and washed with N, N-dimethyl formamide, ethanol and ether, respectively. The collected solid was then dried in vacuo overnight to yield **TAT-COF** (48.4 mg, 91.7% yield). IR (KBr pellet cm^{-1}): 3384 (w), 3026 (w), 1700 (w), 1670 (w), 1596 (w), 1576 (w), 1515 (vs), 1447 (vw), 1413 (w), 1367 (s), 1293 (w), 1198 (w), 1105 (vw), 1014 (w), 810 (s), 742 (w), 688 (w), 548 (w).

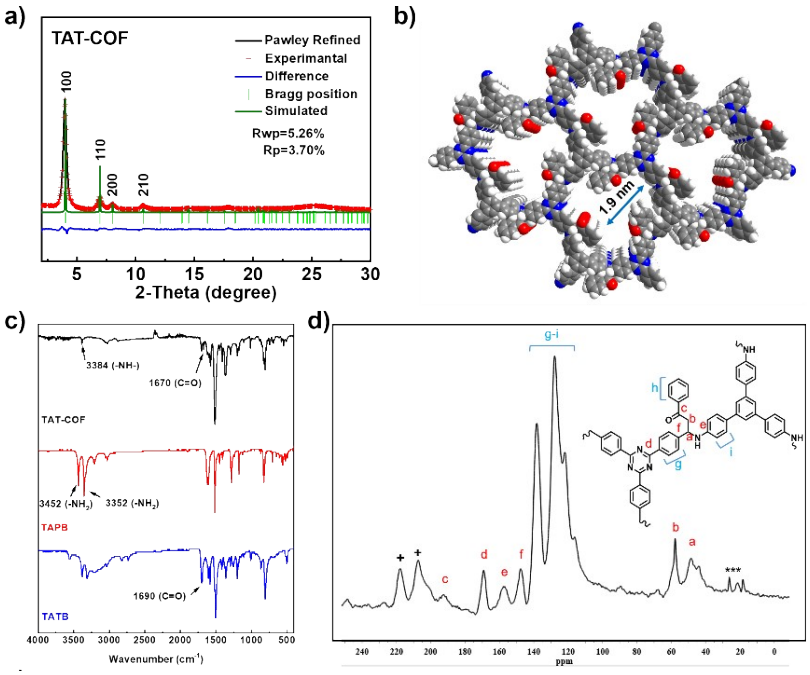

Fig. S8 a) PXRD patterns of **TAT-COF** (AA stacking). b) The top and side views of **TAT-COF** (AA stacking). c) The FT-IR spectra of **TAT-COF** and its part monomers. The FT-IR spectra showed the characteristic peaks such as 1670 cm^{-1} for [−C=O], 3384 cm^{-1} for [−N-H] stretching vibrations, which

suggested the formation of **TAT-COF** through Mannich condensation reaction. d) The solid-state ^{13}C-MAS NMR spectrum of **TAT-COF**, δ (ppm): 193.0, 169.1, 157.6, 147.6, 138.3, 127.9, 121.9, 57.7, 48.8. The formation of **TAT-COF** was verified by the existence of the keto and aliphatic carbon in **TAT-COF** through the corresponding resonances at 193.0, 57.7, 48.8 ppm, respectively. e) The solid-state ^{15}N NMR spectrum of **TAT-COF**, δ (ppm): 328.9, 126.8, 52.3. The formation of **TAT-COF** was verified by the existence of the nitrogen in triazine and β-Ketamine in **TAT-COF** through the corresponding resonances at 328.9 and 126.8 ppm, respectively. f) N_2 adsorption isotherms for **TAT-COF** at 77 K. N_2 adsorption at 77 K revealed absorption amounts of **TAT-COF** was 300.0 cm^3/g, and its surface areas calculated on basis of the BET model were determined as 783.0 m^2/g. g) Pore size distribution curve of **TAT-COF**. Pore size distribution curves, calculated from nonlocal density functional theory (NLDFT) analysis, showed that the pore width of **TAT-COF** was centered at ~1.7 nm. h) SEM image of **TAT-COF**. i) SEM-EDX images of **TAT-COF**. j) TEM image of the **TAT-COF**. k) TGA trace of **TAT-COF** measured under nitrogen flow with a heating rate 10 °C/min up to 800 °C, which can be stable up to 420 °C. l) UV-Vis curve of the **TAT-COF** measured in solid state. **TAT-COF** exhibited three absorption peaks at around 280, 350 and 435 nm with an absorbance edge at 700 nm. m) Photocurrent response of **TAT-COF**.

Table S4. Fractional atomic coordinates for the unit cell of **TAT-COF**

TAT-COF AA stacking mode, space group: *P3*

$a = b = 25.4243$ Å, $c = 4.3467$ Å

$\alpha = \beta = 90°$, $\gamma = 120°$

Aotm	x	y	z
H1	0.48975	0.70392	0.30101
H2	0.59498	0.78317	0.28471
H3	0.44088	0.82814	0.7101
H4	0.6099	0.95297	0.18858
H5	0.75409	0.84047	0.13826
H6	0.86081	0.87706	0.25261
H7	0.86092	1.00698	0.89333
H8	0.75538	0.97102	0.776
H9	0.77883	1.03175	0.2368
H10	0.88175	1.11525	0.30687
H11	0.90254	1.20171	0.64649
H12	0.81788	1.20355	0.91838
H13	0.71334	1.11975	0.85808
H14	1.11217	1.04714	0.61194
C15	1.31876	-0.39268	-0.4908
N16	1.37786	-0.34782	-0.49104
C17	1.30301	-0.45702	-0.49693

C18	1.24685	-0.50174	-0.61401
C19	1.23241	-0.56241	-0.62692
C20	1.27404	-0.57995	-0.52333
C21	1.32935	-0.53502	-0.39629
C22	1.34403	-0.47427	-0.38688
C23	1.26	-0.64586	-0.52796
C24	1.31004	-0.65305	-0.69691
N25	1.20054	-0.68668	-0.66814
C26	1.34471	-0.67227	-0.48633
C27	1.33176	-0.73635	-0.45854
O28	1.38629	-0.63273	-0.33691
C29	1.28312	-0.78524	-0.61441
C30	1.27138	-0.8447	-0.57475
C31	1.30836	-0.85645	-0.38367
C32	1.35712	-0.80872	-0.23098
C33	1.36868	-0.74923	-0.26686
C34	1.15694	-0.74617	-0.55593
C35	1.09918	-0.77675	-0.69146
C36	1.05898	-0.83775	-0.62448
C37	1.07582	-0.86956	-0.41956
C38	1.13225	-0.83804	-0.27056
C39	1.17208	-0.7769	-0.33571
C40	1.0369	-0.93622	-0.38171
C41	1.06323	-0.97338	-0.37908
H42	1.25852	-0.65776	-0.28413
H43	1.29059	-0.68573	-0.88715
H44	1.1919	-0.67487	-0.88483
H45	1.36159	-0.54683	-0.30465

12. Reference

1. P. F. Wei, M. Z. Qi, Z. P. Wang, S. Y. Ding, W. Yu, Q. Liu, L. K. Wang, H. Z. Wang, W. K. An, W. Wang, *J. Am. Chem. Soc.*, 2018, **140**, 4623-4631.
2. D. Meng, J. Xue, Y. F. Zhang, T. J. Liu, C. C. Chen, W. J. Song, J. C. Zhao, *Catal. Sci. Technol.*, 2023, **13**, 1518-1526.

3. Z. J. Wang, R. Li, K. Landfester, K. A. Zhang, *Polymer.*, 2017, **126**, 291-295.
4. J. Luo, X. Zhang, J. Zhang, *ACS Catal.*, 2015, **5**, 2250-2254.
5. X.-L. Yan, H. Liu, Y.-S. Li, W.-B. Chen, T. Zhang, Z.-Q. Zhao, G.-L. Xing, L. Chen, *Macromolecules.*, 2019, **52**, 7977-7983.
6. S.-F. Liu, Z.-Q. Liu, Q. Su, Q.-L. Wu, *Micropor. Mesopor. Mater.*, 2022, **333**, 111737.
7. G.-B. Wang, Y.-J. Wang, J.-L. Kan, K.-H. Xie, H.-P. Xu, F. Zhao, M.-C. Wang, Y. Geng and Y.-B. Dong, *J. Am. Chem. Soc.*, 2023, **145**, 4951−4956.